

Reaction Properties of the *trans*-Hyponitrite Complex [Ru₂(CO)₄(μ-H)(μ-PBu_t)₂(μ-Ph₂PCH₂PPh₂)(μ-η²-ONNO)]

Hans-Christian Böttcher* and Christoph Wagner

*Institute of Inorganic Chemistry, Martin Luther University Halle-Wittenberg,
Kurt-Mothes-Strasse 2, D-06120 Halle/Saale, Germany*

Karl Kirchner

*Institute of Applied Synthetic Chemistry, Vienna University of Technology, Getreidemarkt 9,
A-1060 Vienna, Austria*

Received March 18, 2004

The protonation of [Ru₂(CO)₄(μ-H)(μ-PBu_t)₂(μ-dppm)(μ-η²-ONNO)] (**1**) with HBF₄ occurs at the oxygen of the noncoordinating side of the *trans*-hyponitrite ligand to give [Ru₂(CO)₄(μ-H)(μ-PBu_t)₂(μ-dppm)(μ-η²-ONNOH)][BF₄] (**2**) in good yield. The monoprotonated hyponitrite in **2** is deprotonated easily by strong bases to regenerate **1**. Furthermore, **1** reacts with the methylating reagent [Me₃O][BF₄] to afford [Ru₂(CO)₄(μ-H)(μ-PBu_t)₂(μ-dppm)(μ-η²-ONNOMe)][BF₄] (**3**). The molecular structures of **2** and **3** have been determined crystallographically, and the structure of **2** is discussed with the results of the DFT/B3LYP calculations on the model complex [Ru₂(CO)₄(μ-H)(μ-PH₂)(μ-H₂PCH₂PH₂)(μ-η²-ONNOH)]⁺ (**2a**). Moreover, the thermolysis of **2** in ethanol affords [Ru₂(CO)₄(μ-H)(μ-OH)(μ-PBu_t)₂(μ-dppm)][BF₄] (**4**) in high yield, and the deprotonation of **4** by DBU in THF yields the novel complex [Ru₂(CO)₄(μ-OH)(μ-PBu_t)₂(μ-dppm)] (**5**).

Introduction

Recently, we reported the synthesis and the X-ray crystal structure of the *trans*-hyponitrite complex [Ru₂(CO)₄(μ-H)(μ-PBu_t)₂(μ-dppm)(μ-η²-ONNO)] (**1**, dppm = Ph₂PCH₂PPh₂), which was obtained by the reductive dimerization of nitric oxide in the coordination sphere of the coordinatively unsaturated compound [Ru₂(CO)₄(μ-H)(μ-PBu_t)₂(μ-dppm)].¹ In the solid state, **1** exhibits a very close intramolecular contact between one C atom of a carbonyl group and the noncoordinating O atom of the *trans*-hyponitrite ligand. Therefore, we postulated that the latter should be a center of high nucleophilicity for the addition of electrophiles. Therein, we describe further studies in this field, for example, reactions of complex **1** with electrophilic reagents such as HBF₄ and CH₃⁺ (from [Me₃O][BF₄]) that yield the complex salts [Ru₂(CO)₄(μ-H)(μ-PBu_t)₂(μ-dppm)(μ-η²-ONNOX)][BF₄] (X = H for **2**; X = CH₃ for **3**). Furthermore, the reaction behavior of **2** and **3** under thermolytic conditions was investigated.

* Author to whom correspondence should be addressed. E-mail: boettcher@chemie.uni-halle.de.

(1) Böttcher, H.-C.; Graf, M.; Mereiter, K.; Kirchner, K. *Organometallics* 2004, 23, 1269.

Experimental Section

General Information. All synthetic operations were performed under a dry argon atmosphere using conventional Schlenk techniques. Solvents were dried in the presence of sodium benzophenone ketyl or molecular sieves and distilled under argon prior to use. Compound **1** was prepared as described previously.¹ Tetrafluoroboric acid, trimethylxonium tetrafluoroborate, and DBU were purchased commercially. IR spectra were recorded as KBr pellets on a Mattson 5000 FTIR spectrometer. NMR spectra were obtained on Varian Unity 400 MHz or Varian Gemini 200 MHz equipment. Chemical shifts are given in parts per million from SiMe₄ (¹H) or 85% H₃PO₄ (³¹P{¹H}). Microanalyses (C, H, and N) were performed by the University of Halle's microanalytical laboratory.

[Ru₂(CO)₄(μ-H)(μ-PBu_t)₂(μ-dppm)(μ-η²-ONNOH)][BF₄] (**2**). A stirred slurry of [Ru₂(CO)₄(μ-H)(μ-PBu_t)₂(μ-dppm)(μ-η²-ONNO)] (**1**) (452 mg, 0.5 mmol) in THF (30 mL) was treated with a few drops of tetrafluoroboric acid (aqueous, 40%) at room temperature. The color of the suspension changed from deep yellow to pale yellow, and a clear solution was obtained immediately. After the solution was stirred for ~30 min, the solvent was removed in vacuo. The residue was dissolved in 5 mL of acetone, and **2** was precipitated by the addition of diethyl ether (40 mL). The cream-colored solid was filtered off, washed twice with 20 mL of diethyl ether, and dried in vacuo. Yield: 452 mg (91%). Mp: 129–131

°C dec. Anal. Calcd for C₃₇H₄₂BF₄N₂O₆P₃Ru₂: C, 44.78; H, 4.27; N, 2.82. Found: C, 45.01; H, 4.69; N, 3.21. IR (KBr): ν(OH) 3223 (br); ν(CO) 2054 (sh), 2046 (sh), 2039 (vs), 1999 (vs), 1985 (vs); ν(NN) 1484 (s), 1435 (s); ν(NO) 1088 (s), 1054 (s), 1019 (s), 971 (s) cm⁻¹. ¹H NMR (CDCl₃): δ 11.13 (s, 1H, NOH), 7.76–7.11 (m, 20H, PC₆H₅), 3.06 (m, 1H, P–CH₂–P), 1.90 (m, 1H, P–CH₂–P), 1.55 (d, 18H, ³J_{PH} = 14.3 Hz, PC₄H₉), –12.62 (m, 1H, μ-H). ³¹P{¹H} NMR (CDCl₃): δ 274.9 (dd, ²J_{PP} = 187.8 Hz, ²J_{PP} = 147.3 Hz, μ-PBu₂′), 42.6 (dd, ²J_{PP} = 147.3 Hz, ²J_{PP} = 62.3 Hz, PC₆H₅), 37.5 (dd, ²J_{PP} = 62.3 Hz, ²J_{PP} = 187.2 Hz, PC₆H₅). The following IR hyponitrite bands (not published in ref 1) have been assigned for **1** (KBr): ν(NN) 1482 (m), 1434 (s); ν(NO) 1099 (m), 1041 (m), 1025 (m), 971 (m) cm⁻¹.

[Ru₂(CO)₄(μ-H)(μ-PBu₂′)(μ-dppm)(μ-η²-ONNOMe)][BF₄] (**3**). To a stirred solution of [Ru₂(CO)₄(μ-H)(μ-PBu₂′)(μ-dppm)(μ-η²-ONNO)] (452 mg, 0.5 mmol) in dichloromethane (30 mL) was added solid trimethyloxonium tetrafluoroborate (74 mg, 0.5 mmol) at room temperature. Within ~15 min, the color of the solution changed slowly from deep yellow to pale yellow. After the solution was stirred for 45 min, the solvent was removed in vacuo. The remaining residue was dissolved in 5 mL of dichloromethane, and 30 mL of ethanol was added. Then, the solvent was reduced to 5 mL in vacuo, and **3** was obtained as pale yellow plates by cooling at 5 °C overnight. The crystals were filtered off, washed twice with 10 mL of diethyl ether, and dried in vacuo. Yield: 398 mg (79%). Mp: 120–122 °C dec. Anal. Calcd for C₃₈H₄₄BF₄N₂O₆P₃Ru₂: C, 45.34; H, 4.41; N, 2.78. Found: C, 44.98; H, 4.70; N, 2.55. IR (KBr): ν(CO) 2061 (sh), 2053 (vs), 2000 (vs), 1973 (vs); ν(NN) 1468 (m), 1433 (s); ν(NO) 1094 (s), 1025 (m), 999 (m), 958 (m) cm⁻¹. ¹H NMR (CDCl₃): δ 7.99–7.11 (m, 20H, PC₆H₅), 3.62 (m, 1H, P–CH₂–P), 3.10 (s, 3H, O–CH₃), 1.81 (m, 1H, P–CH₂–P), 1.54 (d, 18H, ³J_{PH} = 14.2 Hz, PC₄H₉), –12.55 (m, 1H, μ-H). ³¹P{¹H} NMR (CDCl₃): δ 278.0 (dd, ²J_{PP} = 186.2 Hz, ²J_{PP} = 143.7 Hz, μ-PBu₂′), 43.4 (dd, ²J_{PP} = 143.4 Hz, ²J_{PP} = 60.5 Hz, PC₆H₅), 39.3 (dd, ²J_{PP} = 60.5 Hz, ²J_{PP} = 186.2 Hz, PC₆H₅).

Deprotonation of [Ru₂(CO)₄(μ-H)(μ-PBu₂′)(μ-dppm)(μ-η²-ONNOH)][BF₄] with DBU. To a stirred slurry of **2** (496 mg, 0.5 mmol) in THF (20 mL) was added DBU (0.1 mL, excess). The suspension changed immediately to a yellow solution, which was stirred additionally for ~15 min. The solvent was removed under reduced pressure, and ³¹P NMR investigation of the remaining residue (CDCl₃) showed the formation of **1** as the only phosphorus-containing product indicated by its characteristic data.¹

[Ru₂(CO)₄(μ-H)(μ-OH)(μ-PBu₂′)(μ-dppm)(μ-η²-ONNOH)][BF₄] (**4**). A solution of [Ru₂(CO)₄(μ-H)(μ-PBu₂′)(μ-dppm)(μ-η²-ONNOH)][BF₄] (496 mg, 0.5 mmol) was refluxed in ethanol (20 mL) for 1 h. During this time, the color of the solution changed from pale yellow to deep yellow. After the solution was cooled to room temperature and the solvent removed in vacuo, the remaining residue was dissolved in a minimum of acetone and analytically pure **4** was obtained by the addition of diethyl ether (50 mL) with vigorous stirring. The pale-yellow crystals were filtered off, washed with 20 mL of diethyl ether, and dried in vacuo. Yield: 408 mg (86%). Mp: 240–242 °C dec. Anal. Calcd for C₃₇H₄₂BF₄O₆P₃Ru₂: C, 46.83; H, 4.46; P, 9.80. Found: C, 46.63; H, 4.52; P, 10.03. IR (KBr): ν(OH) 3576 (s br); ν(CO) 2044 (vs), 2025 (vs), 1984 (vs), 1970 (vs) cm⁻¹. ¹H NMR (CDCl₃): δ 7.54–7.19 (m, 20H, PC₆H₅), 2.64 (m, 1H, P–CH₂–P), 1.87 (m, 1H, P–CH₂–P), 1.58 (d, 9H, ³J_{PH} = 14.1 Hz, PC₄H₉), 1.49 (d, 9H, ³J_{PH} = 14.5 Hz, PC₄H₉), –0.04 (d br, 1H, μ-OH, ³J_{PH} = 3.4 Hz), –11.14 (m, 1H, μ-H). ³¹P{¹H} NMR (CDCl₃): δ 228.6 (t, ²J_{PP} = 183.8 Hz, μ-PBu₂′), 43.1 (d, ²J_{PP} = 183.8 Hz, PC₆H₅).

[Ru₂(CO)₄(μ-OH)(μ-PBu₂′)(μ-dppm)] (**5**). A stirred solution of [Ru₂(CO)₄(μ-H)(μ-OH)(μ-PBu₂′)(μ-dppm)][BF₄] (474 mg, 0.5 mmol) in THF (20 mL) was treated with 0.1 mL (excess) of DBU. The color of the solution turned immediately from light yellow to deep yellow. After the solution was stirred for 15 min, the solvent was removed in vacuo. The remaining residue was dissolved in 3 mL of dichloromethane, and 30 mL of hexane was added while **5** precipitated as bright-yellow crystals. Yield: 349 mg (81%). Mp: 188–192 °C dec. Anal. Calcd for C₃₇H₄₁O₆P₃Ru₂: C, 51.63; H, 4.80; P, 10.79. Found: C, 51.89; H, 4.88; P, 10.53. IR (KBr): ν(OH) 3654 (m); ν(CO) 1992 (vs), 1969 (vs), 1923 (vs), 1909 (vs) cm⁻¹. ¹H NMR (CDCl₃): δ 7.55–7.01 (m, 20H, PC₆H₅), 2.98 (m, 1H, P–CH₂–P), 2.60 (m, 1H, P–CH₂–P), 1.62 (d, 9H, ³J_{PH} = 13.5 Hz, PC₄H₉), 1.45 (d, 9H, ³J_{PH} = 11.7 Hz, PC₄H₉), –1.57 (m, 1H, μ-OH). ³¹P{¹H} NMR (CDCl₃): δ 249.4 (t, ²J_{PP} = 173.9 Hz, μ-PBu₂′), 29.5 (d, ²J_{PP} = 173.9 Hz, PC₆H₅).

Reaction of [Ru₂(CO)₄(μ-OH)(μ-PBu₂′)(μ-dppm)] with HBF₄. A stirred solution of [Ru₂(CO)₄(μ-OH)(μ-PBu₂′)(μ-dppm)] (215 mg, 0.25 mmol) was treated with a few drops of tetrafluoroboric acid (aqueous, 40%) at room temperature. The color of the solution changed spontaneously from deep yellow to pale yellow. After the solution was stirred for 15 min, the solvent was removed in vacuo and ³¹P NMR investigation of the residue in the CDCl₃ solution showed the formation of **4** as the only phosphorus-containing product.

Computational Details. The DFT calculations were performed using the Gaussian98 software package on the Silicon Graphics Origin 2000 of the Vienna University of Technology.² The geometry and energy of the model complex were optimized at the B3LYP level³ of theory with the Stuttgart/Dresden ECP (SDD) basis set⁴ to describe the electrons of the ruthenium atom. For all of the other atoms, the 6-31g** basis set was employed.⁵ A vibrational analysis was performed to confirm that the structure has no imaginary frequencies. The geometry was optimized without constraints (C₁ symmetry).

X-ray Structure Determination for 2 and 3. Crystals of **2** were obtained by the slow diffusion of diethyl ether into an acetone solution at room temperature. Suitable crystals of **3** were grown from ethanol at 5 °C overnight. Crystal data and experimental details are given in Table 1. X-ray data were collected on a Stoe-IPDS

- (2) Frisch, M. J.; Trucks, G. W.; Schlegel, H. B.; Scuseria, G. E.; Robb, M. A.; Cheeseman, J. R.; Zakrzewski, V. G.; Montgomery, J. A., Jr.; Stratmann, R. E.; Burant, J. C.; Dapprich, S.; Millam, J. M.; Daniels, A. D.; Kudin, K. N.; Strain, M. C.; Farkas, O.; Tomasi, J.; Barone, V.; Cossi, M.; Cammi, R.; Mennucci, B.; Pomelli, C.; Adamo, C.; Clifford, S.; Ochterski, J.; Petersson, G. A.; Ayala, P. Y.; Cui, Q.; Morokuma, K.; Malick, D. K.; Rabuck, A. D.; Raghavachari, K.; Foresman, J. B.; Cioslowski, J.; Ortiz, J. V.; Stefanov, B. B.; Liu, G.; Liashenko, A.; Piskorz, P.; Komaromi, I.; Gomperts, R.; Martin, R. L.; Fox, D. J.; Keith, T.; Al-Laham, M. A.; Peng, C. Y.; Nanayakkara, A.; Gonzalez, C.; Challacombe, M.; Gill, P. M. W.; Johnson, B.; Chen, W.; Wong, M. W.; Andres, J. L.; Head-Gordon, M.; Replogle, E. S.; Pople, J. A. *Gaussian 98*, revision A.7; Gaussian, Inc.: Pittsburgh, PA, 1998.
- (3) (a) Becke, A. D. *J. Chem. Phys.* **1993**, *98*, 5648. (b) Miehlich, B.; Savin, A.; Stoll, H.; Preuss, H. *Chem. Phys. Lett.* **1989**, *157*, 200. (c) Lee, C.; Yang, W.; Parr, G. *Phys. Rev. B* **1988**, *37*, 785.
- (4) (a) Haeusermann, U.; Dolg, M.; Stoll, H.; Preuss, H. *Mol. Phys.* **1993**, *78*, 1211. (b) Kuechle, W.; Dolg, M.; Stoll, H.; Preuss, H. *J. Chem. Phys.* **1994**, *100*, 7535. (c) Leininger, T.; Nicklass, A.; Stoll, H.; Dolg, M.; Schwerdtfeger, P. *J. Chem. Phys.* **1996**, *105*, 1052.
- (5) (a) McClean, A. D.; Chandler, G. S. *J. Chem. Phys.* **1980**, *72*, 5639. (b) Krishnan, R.; Binkley, J. S.; Seeger, R.; Pople, J. A. *J. Chem. Phys.* **1980**, *72*, 650. (c) Wachters, A. J. H. *J. Chem. Phys.* **1970**, *52*, 1033. (d) Hay, P. J. *J. Chem. Phys.* **1977**, *66*, 4377. (e) Raghavachari, K.; Trucks, G. W. *J. Chem. Phys.* **1989**, *91*, 1062. (f) Binning, R. C.; Curtiss, L. A. *J. Comput. Chem.* **1995**, *103*, 6104. (g) McGrath, M. P.; Radom, L. *J. Chem. Phys.* **1991**, *94*, 511.

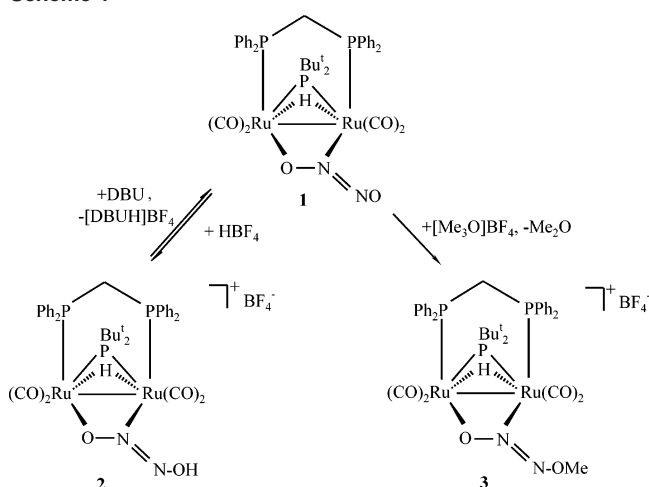
Table 1. Details for the Crystal Structure Determination of Complexes **2** and **3**

	2	3
formula	C ₃₇ H ₄₁ BF ₄ N ₂ O ₆ P ₃ Ru ₂	C ₃₈ H ₄₄ BF ₄ N ₂ O ₆ P ₃ Ru ₂
fw	991.58	1006.61
cryst size (mm)	0.30 × 0.36 × 0.36	0.42 × 0.27 × 0.09
cryst syst	monoclinic	triclinic
space group	<i>P</i> 2 ₁ / <i>n</i>	<i>P</i> 1
<i>a</i> (Å)	17.250(3)	11.863(2)
<i>b</i> (Å)	12.404(2)	12.561(3)
<i>c</i> (Å)	19.829(4)	14.876(3)
α (deg)		94.03(2)
β (deg)	96.18(2)	99.15(2)
γ (deg)		98.15(2)
<i>V</i> (Å ³)	4218.2(13)	2156.5(7)
<i>Z</i>	4	2
ρ_{calc} (g cm ⁻³)	1.561	1.550
<i>T</i> (K)	220(2)	220(2)
μ (mm ⁻¹) (Mo K α)	0.892	0.874
<i>F</i> (000)	1996	1016
abs corr	numerical	numerical
θ range for data	2.03–25.99	2.22–25.97
collection (deg)		
no. of rflns	31184	14986
no. of unique rflns	8118 (<i>R</i> _{int} = 0.0577)	7821 (<i>R</i> _{int} = 0.0316)
no. of rflns (<i>I</i> > 2 σ (<i>I</i>))	7335	6454
no. of params	633	711
<i>R</i> 1, w <i>R</i> 2 (<i>I</i> > 2 σ (<i>I</i>))	0.0309, 0.0821	0.0328, 0.0950
<i>R</i> 1, w <i>R</i> 2 (all data)	0.0347, 0.0846	0.0441, 0.1178
residual electron	0.955, -0.665	0.931, -1.355
density (e Å ⁻³)		

diffractometer (graphite monochromated Mo K α radiation, with $\lambda = 0.71073$ Å). Corrections for Lorentz and polarization effects, crystal decay, and absorption were applied. The structures were solved by direct methods using the SHELXS97 program.⁶ Structure refinement on *F*² was carried out with the SHELXL97 program.⁷ All non-hydrogen atoms were refined anisotropically. The positions of the hydrogen atoms were located from the Fourier map and refined isotropically. The fluorine atoms of the tetrafluoroborate of **3** were found to be disordered; that is, along the F1–B axis, the positions of F2, F3, and F4 are found with free refined occupation factors of 70 and 30%.

Results and Discussion

Treatment of the coordinatively unsaturated species [M₂(CO)₄(μ -H)(μ -PBU'₂)(μ -dppm)] (M = Fe or Ru) with strong acids, such as HBF₄, results in rapid protonation of the dimetal vector to give the corresponding complex salt [M₂(CO)₄(μ -H)₂(μ -PBU'₂)(μ -dppm)][BF₄]. For the closely related compound [Ru₂(CO)₄(μ -Cl)(μ -PBU'₂)(μ -dppm)], an analogous reaction behavior is observed; thus its protonation affords [Ru₂(CO)₄(μ -H)(μ -Cl)(μ -PBU'₂)(μ -dppm)][BF₄].⁸ For the hyponitrite complex [Ru₂(CO)₄(μ -H)(μ -PBU'₂)(μ -dppm)(μ - η^2 -ONNO)] (**1**), essentially two possible pathways during the reaction with acids are conceivable: (i) protonation of the metal–metal bond or (ii) protonation of the hyponitrite ligand (on O and N). Since **1** possesses a center of high nucleophilicity at the noncoordinating oxygen of the *trans*-hyponitrite, the second reaction pathway should be favored

Scheme 1

clearly. Indeed, treatment of **1** with tetrafluoroboric acid in THF leads to a clean protonation of its *trans*-hyponitrite ligand to give the complex salt [Ru₂(CO)₄(μ -H)(μ -PBU'₂)(μ -dppm)(μ - η^2 -ONNO)][BF₄] (**2**) in high yield (Scheme 1). No further products could be detected spectroscopically. Complex **2** is obtained analytically pure by crystallization from acetone/diethyl ether as pale-yellow crystals, which are stable in air. The molecular structure of **2** has been elucidated by single-crystal X-ray structure analysis (see below). A comparison of the IR spectra (KBr) of **1** and **2** affords a remarkable difference. The spectrum of **2** contains only absorption bands that are characteristic of terminal carbonyls; for example, there is no band in the region that corresponds to bridging carbonyls, which is caused in **1** by the interaction of a carbonyl carbon with the noncoordinating oxygen atom of the hyponitrite ligand (1742 cm⁻¹).¹ In general, a shift to higher wavenumbers for the carbonyls is observed in the spectrum, indicating that the negative charge on the noncoordinating NO group in the educt **1** is offset obviously in the product of **2**. Furthermore, a broad band at 3223 cm⁻¹ indicates the presence of a hydroxy group. In the ¹H NMR spectrum, a signal corresponding to the NOH group at 11.13 ppm is found and this singlet disappears by the treatment of CDCl₃ solutions of the compound with D₂O. Therefore, the assignment of the signal should be correct. Furthermore, the chemical shift of the latter signal is in good accordance with those found for *N*-alkyl-*N'*-hydroxydiazene-*N*-oxides (11–12 ppm).⁹ The ¹H NMR spectroscopic data of **2** include a characteristic resonance at -12.62 ppm as a multiplet which can be attributed to a bridging hydrido ligand. The relative areas of the signals in the proton spectrum show unambiguously the presence of only one hydride. The ³¹P{¹H} NMR spectrum of **2** indicates the chemical inequivalence of the two phosphorus nuclei of the bridging dppm ligand. They give rise to two signals (dd) with corresponding couplings to the phosphorus of the phosphido bridge (dd).

The result of the structural identification of **2**, established by X-ray crystallography, afforded unambiguously the pre-

(6) Sheldrick, G. M. *SHELXS97: Program for the Solution of Crystal Structures*; University of Göttingen: Göttingen, Germany, 1997.

(7) Sheldrick, G. M. *SHELXL97: Program for Crystal Structure Refinement*; University of Göttingen: Göttingen, Germany, 1997.

(8) Böttcher, H.-C.; Graf, M.; Merzweiler, K.; Wagner, C. J. *Organomet. Chem.* **2001**, *628*, 144.

(9) Arulsamy, N.; Bohle, D. S.; Imonigie, J. A.; Sagan, E. S. *J. Am. Chem. Soc.* **2000**, *122*, 5539 and references therein.

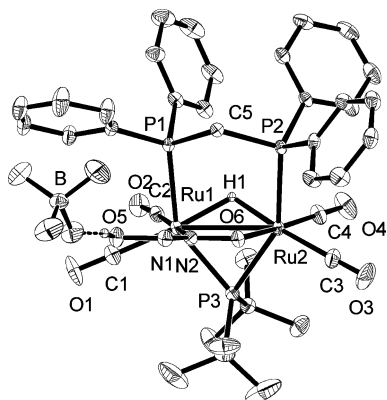


Figure 1. Perspective view of the molecular structure of [Ru₂(CO)₄(μ-H)(μ-PBu₂)(μ-dppm)(μ-η²-ONNOH)][BF₄] (**2**) in the crystal showing 30% thermal displacement ellipsoids. Selected bond lengths and angles are in Table 2.

Table 2. Observed Parameters and Computational Results (in Å and deg) for Complexes **1–3** and the Model Complex **2a**

	1 solv (obsd) complex 1 ^a	2 (obsd)	2a (calcd)	3 (obsd)
Ru(1)–Ru(2)	2.8479(2)	2.8632(5)	2.874	2.8254(7)
Ru(1)–N(2)	2.060(2)	2.116(2)	2.163	2.112(3)
Ru(1)–C(1)	1.944(2)	1.915(3)	1.933	1.913(4)
Ru(1)–C(2)	1.883(2)	1.892(3)	1.908	1.890(4)
Ru(1)–H(1)	1.743(9)		1.773	
Ru(2)–O(6)	2.125(2)	2.1105(17)	2.131	2.108(3)
Ru(2)–C(3)	1.909(2)	1.907(3)	1.938	1.913(4)
Ru(2)–C(4)	1.874(2)	1.868(3)	1.898	1.854(4)
Ru(2)–H(1)	1.743(9)		1.759	
N(2)–O(6)	1.357(2)	1.341(3)	1.328	1.333(4)
N(1)–N(2)	1.261(2)	1.261(3)	1.252	1.262(5)
N(1)–O(5)	1.313(3)	1.381(3)	1.381	1.384(5)
O(5)–H(2)		0.72(4)	0.971	
O(5)–C(38)				1.468(7)
N(1)–N(2)–O(6)	115.5(2)	111.4(2)	113.2	110.5(3)
N(2)–N(1)–O(5)	112.5(2)	109.2(2)	109.4	107.7(3)
Ru(1)–C(1)–O(1)	158.9(2)	174.1(3)		175.4(4)

^a Data of the two independent molecules of **1**; see ref 1.

sense of a monoprotonated hyponitrite in a trans configuration. A representation of the cation of **2** with the corresponding tetrafluoroborate is shown in Figure 1, and selected bond lengths and angles are summarized in Table 2. The cation of the compound consists of a diruthenium tetracarbonyl core bridged by a hydrido, a phosphido group, the dppm, and the monoprotonated hyponitrite ligand. The structural data agree very well with the observed bonding characteristics of **1**. This supports, again, the correctness of the structure analysis of **1** since, despite the accuracy of the structure determination, there were perceptible consequences of solvent disorder phenomena for this compound.¹ Therefore, for comparative purposes, some important bonding parameters of **1** are listed additionally in Table 2. Regardless of the abnormalities concerning the specific bonding situation of the carbonyl ligand [C(1)–O(1)] in **1**, there is very good accordance in the structural parameters of **1** and **2**. As depicted in Figure 1, for **2** in the solid state, a considerable extent of hydrogen bonding between the hydroxy group at the nitrogen and the corresponding tetrafluoroborate can be discussed. The oxygen atom of the related hydroxy group interacts with one fluorine atom of the tetrafluoroborate with

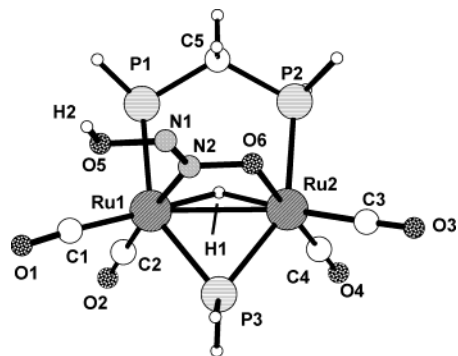


Figure 2. Optimized geometry for the model complex [Ru₂(CO)₄(μ-H)(μ-PH₂)(μ-H₂PCH₂PH₂)(μ-η²-ONNOH)]⁺ (**2a**) calculated at the B3LYP (Ru sdd; C, H, N, O, P 6-31g**) level of theory. Selected bond lengths and angles are in Table 2.

the F(3)···O(5) bond distance of 2.661 Å; therefore, it is reasonable to assume strong hydrogen bonding.

Furthermore, DFT/B3LYP calculations, carried out to evaluate the most likely site of protonation in **1**, confirmed that protonation takes place exclusively on the noncoordinating O atom of the ONNO ligand. Accordingly, the model complex cation [Ru₂(CO)₄(μ-H)(μ-PH₂)(μ-H₂PCH₂PH₂)(μ-η²-ONNOH)]⁺ (**2a**) is the only reasonably stable entity. The geometric parameters of **2a** are in very good agreement with the X-ray crystal-structure data of the complex cation of **2**, despite the absence of substituents in the model complex (Table 2). The optimized geometry of **2a** is shown in Figure 2.

To investigate the acid–base character of the latter reaction, we proved the behavior of **2** toward strong bases (e.g., DBU). By this way, a deprotonation was realized by treating **2** with DBU at room temperature. Thus, a suspension of the compound in THF changed immediately to a yellow solution by the addition of a base, and NMR investigations showed unambiguously the transformation of **2** back into **1**.

Furthermore, we were interested in the chemical reactivity of the hyponitrite ligand in **1** toward alkylating reagents. In principle, for N₂O₂²⁻, the alkylating reactions could produce no less than six isomers because of hyponitrite's ambidentate nucleophilic behavior coupled with a facile *E/Z* isomerization. In this context, reactions of the dialkylation of silver hyponitrite have been well demonstrated.⁹ In analogy to the protonation of **1**, an alkylation of the noncoordinating O atom should occur with certainty; however, reaction at the nitrogen, resulting in the formation of a *N*-alkyl-*N'*-diazene-*N*-oxide derivative, could not be ruled out. First attempts using methyl iodide as the methylating reagent resulted in a mixture of products. Consequently, we used Meerwein's salt to realize a cleaner conversion. Thus, compound **1** reacts in dichloromethane at room temperature with [Me₃O][BF₄] to afford the complex salt [Ru₂(CO)₄(μ-H)(μ-PBu₂)(μ-dppm)(μ-η²-ONNOMe)][BF₄] (**3**) in high yield (Scheme 1). Compound **3** is obtained as pale-yellow plates by crystallization from acetone/ethyl acetate at room temperature (as ethyl acetate solvate). Recrystallization from ethanol, by cooling to 5 °C overnight, yields **3** as plates without solvent. The alkylation of the noncoordinating oxygen of the hyponitrite ligand is

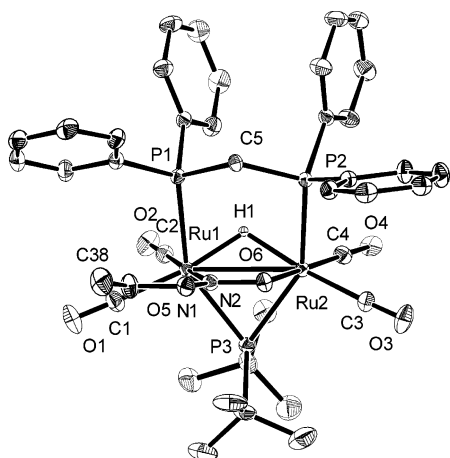
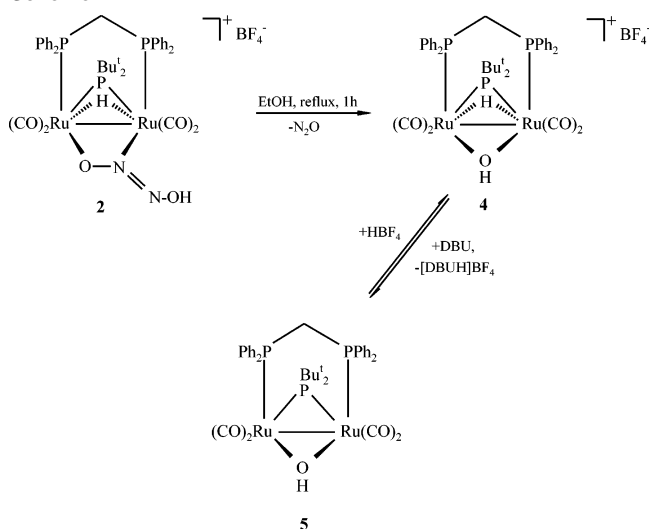


Figure 3. Perspective view of the molecular structure of $[\text{Ru}_2(\text{CO})_4(\mu\text{-H})(\mu\text{-PBu}'_2)(\mu\text{-dppm})(\mu\text{-}\eta^2\text{-ONNOCH}_3)][\text{BF}_4]$ in the crystal showing 30% thermal displacement ellipsoids (tetrafluoroborate omitted for clarity). Selected bond lengths and angles are in Table 2.

indicated clearly by the proton NMR spectrum of **3**, which shows, in comparison with the spectrum of **1**, an additional singlet resonance at 3.10 ppm. Furthermore, the IR spectrum of **3** exhibits the same tendency concerning the position of the carbonyl absorption bands as that observed for **2**; for example, these bands are shifted to higher wavenumbers in comparison with the corresponding bands for **1**. This confirms a decrease in the negative charge of the noncoordinating NO group after alkylation. The ^1H and $^{31}\text{P}\{^1\text{H}\}$ NMR spectra indicate no significant changes in the ligand arrangement of **3** compared with the data of the related complexes **1** and **2**. Additionally, the molecular structure of **3** was confirmed by X-ray crystal-structure analysis. A representation of the molecular structure of the cation of **3** is shown in Figure 3, and selected bond lengths and angles are listed in Table 2. The result of the structure analysis confirmed that the methyl cation generated from Meerwein's reagent exclusively attacks the more negatively charged oxygen atom of the hyponitrite ligand, and therefore no formation of other alkylated products is observed. The structural features of the methylated *trans*-hyponitrite arrangement of **3** are comparable with the structural data found for the *trans-p*-di-*tert*-butylbenzyl hyponitrite molecule, RONNOR ($\text{R} = p\text{-Me}_3\text{CC}_6\text{H}_4\text{CH}_2$).⁹ Thus, the bond distances and angles of the latter compound compare well with the corresponding parameters of **3**: 1.468(2) Å for $\text{C}(1)_{\text{benzyl}}\text{-O}(1)$, 1.361(2) Å for $\text{O}(1)\text{-N}(1)$, and 1.230(3) Å for $\text{N}(1)\text{-N}(1\text{A})$ and $108.29(13)^\circ$ for $\text{C}(1)_{\text{benzyl}}\text{-O}(1)\text{-N}(1)$ and $107.7(2)^\circ$ for $\text{O}(1)\text{-N}(1)\text{-N}(1\text{A})$. Furthermore, the parameters are also in good agreement with the corresponding structural data observed for *trans*-di-*O-tert*-butyl hyponitrite: 1.471(7) Å for $\text{C}_{\text{alkyl}}\text{-O}$, 1.380(6) Å for $\text{O}\text{-N}$, and 1.252(6) Å for $\text{N}\text{-N}$ and $109.3(3)^\circ$ for $\text{C}_{\text{alkyl}}\text{-O}\text{-N}$ and $106.5(3)^\circ$ for $\text{O}\text{-N}\text{-N}$.¹⁰

Compounds **2** and **3** possess (compared to other saltlike complexes) relatively low decomposition points (see Experimental Section). Therefore, we assumed that a decomposition of the hyponitrite ligand resulting in the formation

Scheme 2



of nitrous oxide and hydroxide (e.g., for **2**) should be possible. Studies in this direction concerning compounds of the formula RONNOH were described by other authors.⁹ We found that complex **2** yields (by thermolysis and when the solution is refluxed in ethanol after a short time in a clean manner) only the product $[\text{Ru}_2(\text{CO})_4(\mu\text{-H})(\mu\text{-OH})(\mu\text{-PBu}'_2)(\mu\text{-dppm})][\text{BF}_4]$ (**4**) in high yield (Scheme 2). Complex **4** is obtained analytically pure by crystallization from acetone/diethyl ether as air-stable pale-yellow crystals and was characterized by microanalysis and spectroscopic means. The IR spectrum of **4** contains, in addition to the usually observed four absorption bands that are characteristic of terminal carbonyls, a characteristic $\nu(\text{OH})$ absorption at 3567 cm^{-1} (KBr). This group is indicated additionally in the ^1H NMR spectrum with a resonance signal at -0.09 ppm as a doublet with a coupling to phosphorus at 3.4 Hz. This high-field signal disappeared when D_2O was added to the CDCl_3 solution, and therefore it is assigned unambiguously to the proton of the hydroxo ligand. These characteristic spectroscopic parameters agree well with those found for other hydroxo-bridged ruthenium complexes. For instance, the cluster compounds $[\text{FeRu}_2(\mu\text{-OH})_2(\text{CO})_8\text{L}_2]$ ($\text{L} = \text{PMe}_3$ or AsPh_3) show characteristic IR absorption bands in the region from 3640 to 3570 cm^{-1} , and the corresponding $\mu\text{-OH}$ groups resonate in the proton spectra at -2.16 and -1.78 ppm, respectively.¹¹ Furthermore, the ^1H NMR spectroscopic parameters of **4** include a characteristic resonance at -12.55 ppm as a multiplet that can be attributed to a bridging hydrido ligand.

Moreover, a deprotonation of the metal–metal bond of **4** can be realized by the treatment of THF solutions of the compound with DBU at room temperature. The reaction is indicated by an immediate color change of the solution from pale yellow to deep yellow, and thus the novel complex $[\text{Ru}_2(\text{CO})_4(\mu\text{-OH})(\mu\text{-PBu}'_2)(\mu\text{-dppm})]$ (**5**) is obtained in good yield (Scheme 2). Analytically pure crystals of **5** were grown by crystallization from CH_2Cl_2 /heptane mixtures and were

(10) Ogle, C. A.; Vander Kooi, K. A.; Mendenhall, G. D.; Lorprayoon, V.; Cornilison, B. C. *J. Am. Chem. Soc.* **1982**, *104*, 5114.

(11) Jones, D. F.; Dixneuf, P. H.; Benoit, A.; Le Marouille, J.-Y. *Inorg. Chem.* **1983**, *22*, 29.

characterized by microanalysis and spectroscopic methods. The IR spectrum of **5** exhibits, in addition to the other characteristic absorption bands, a ν(OH) absorption at 3654 cm⁻¹ (KBr), which can be assigned to the bridging hydroxo ligand. The presence of this group is indicated additionally in the ¹H NMR spectrum by a resonance signal at -1.58 ppm as a multiplet with couplings to the other phosphorus nuclei. Like for **4**, this high-field signal disappeared by the treatment of a CDCl₃ solution of **5** with D₂O, indicating unambiguously the hydroxo group. These parameters agree very well with those found for **4** and other similarly constituted complexes.¹¹ On the other hand, complex **5** can be protonated easily in THF by the addition of tetrafluoroboric acid to give back compound **4** in nearly quantitative yield (Scheme 2).

Conclusion

The protonation and alkylation reactions of the hyponitrite ligand of [Ru₂(CO)₄(μ-H)(μ-PBu^t₂)(μ-dppm)(μ-η²-ONNO)] yield exclusively the O-protonated/alkylated species, clearly

demonstrating the nonambidentate nucleophilic behavior of this ligand in the present case. This is well established by the high-yield synthesis and full characterization of the two species [Ru₂(CO)₄(μ-H)(μ-PBu^t₂)(μ-dppm)(μ-η²-ONNOX)]-[BF₄] (X = H for **2**; X = CH₃ for **3**). Under thermolytic conditions, **2** is transformed into the hydroxo-bridged compound [Ru₂(CO)₄(μ-H)(μ-OH)(μ-PBu^t₂)(μ-dppm)][BF₄], which can be deprotonated easily by bases to give the novel complex [Ru₂(CO)₄(μ-OH)(μ-PBu^t₂)(μ-dppm)].

Acknowledgment. We are grateful to the Institut für Anorganische Chemie, Martin-Luther-Universität Halle-Wittenberg for financial support. This paper is dedicated to Professor Reinhard Schmutzler on the occasion of his 70th birthday.

Supporting Information Available: Listings of atomic coordinates, anisotropic temperature factors, and bond lengths and angles for **2** and **3**. This material is available free of charge via the Internet at <http://pubs.acs.org>.

IC0496424